

# Combinatorial and Cross-Fiber Averaging Transform Muscle Electrical Responses with a Large Stochastic Component into Deterministic Contractions

Neil J. Hoover,<sup>1</sup> Adam L. Weaver,<sup>1</sup> Patricia I. Harness,<sup>2</sup> Scott L. Hooper<sup>1</sup>

<sup>1</sup>Neuroscience Program, Department of Biological Sciences, Irvine Hall, Ohio University, Athens, Ohio 45701, and

<sup>2</sup>Neuroscience Doctoral Program, University of California Davis, Davis, California 95616

Pyloric muscles of the stomatogastric neuromuscular system of the lobster *Panulirus interruptus* produce highly deterministic (range, less than  $\pm 6\%$  of mean amplitude) contractions in response to motor nerve stimulation with unchanging spike bursts containing physiological (5–10) spike numbers. Intracellular recordings of extrajunctional potentials (EJPs) evoked in these muscles by motor nerve stimulation revealed a large, apparently stochastic amplitude variation (range,  $\pm 36\%$  of mean amplitude). These observations raised the question of how do electrical responses with a large amplitude variation give rise to deterministic muscle output? We show here that this question is likely resolved by (1) combinatorial averaging within

individual muscle fibers of the multiple EJPs that occur in motor neuron bursts, and (2) averaging across muscle fibers whose electrical responses are uncorrelated. Synapses with high inherent variability are also present in vertebrate CNSs. Combinatorial averaging in multispike inputs would also reduce variation in postsynaptic response at these synapses. The data reported here provide further support that bursting presynaptic activity could make such synapses functionally deterministic as well.

**Key words:** synaptic variation; stomatogastric system; lobster; *Panulirus interruptus*; neuromuscular transform; stochastic; excitatory junctional potential

Nervous systems generate behavior. To perform this task they (1) analyze sensory input; (2) make behavioral choices in light of this input, internal state variables, and past experience; and (3) generate appropriate motor neuron output. The extent to which nervous systems appear to perform these tasks in a deterministic manner—that is, give identical responses to identical inputs—varies as a function of the level of the output being monitored. For instance, primary sensory afferent response to repeated identical stimuli (appropriately timed to avoid synaptic facilitation or depression) is highly stereotyped. Higher cognitive and emotional response to repeated identical input, in contrast, shows much more variability. Nonetheless, a basic tenet of neurobiology is that behavior, cognition, and affect are deterministic functions of nervous system activity, and our inability to predict this output results from our ignorance, not system indeterminacy.

A paradox of this tenet, and the determinism observed in many behaviors, is that nervous system function is inherently probabilistic. For instance, ion channel opening is stochastic, and thus membrane potential shows small variations even at rest. For near-threshold inputs, whether a neuron fires will depend on these stochastic variations because of the all-or-nothing nature of the action potential (Anderson et al., 2000). Similarly, the number of vesicles released per action potential

varies, and these variations can lead to stochastic variation in postsynaptic response to identical presynaptic activity (Allen and Stevens, 1994; Stevens and Wang, 1995; Huang and Stevens, 1997; Simmons, 2000). This variation is not necessarily always deleterious; stochastic variation can increase signal detection to below-threshold sensory input (Douglass et al., 1993; Levin and Miller, 1996; Russell et al., 1999). However, because of its generally destructive effects on information transfer, variation would seem to be deleterious at many stages of sensory and motor processing, and particularly in muscle response to motor neuron activity.

We were therefore surprised when, in the course of investigating the response of lobster (*Panulirus interruptus*) pyloric muscles to motor nerve stimulation, we found that the electrical responses of the muscles [the extrajunctional potentials (EJPs)] had a large, apparently stochastic, amplitude component. These muscles are nonspiking muscles whose contractions are a graded function of motor neuron input (Hoyle, 1953, 1983; Atwood and Hoyle, 1965; Selverston et al., 1976), and this variation would therefore seem to interfere with deterministic control of muscle contraction amplitude by motor neuron activity. However, the amplitude of the muscle contractions induced by stimulating the motor nerves with bursts of action potentials are highly deterministic (Ellis et al., 1996; Morris and Hooper, 1997, 1998; Harness et al., 1998), and these two observations posed the question of how electrical responses with a large-amplitude variation produced highly predictable muscle contractions. We report here that the resolution of this question appears to be a combination of (1) EJP combinatorial averaging within single muscle fibers and (2) averaging across muscle fibers whose electrical responses are uncorrelated.

A preliminary account of these data has appeared in abstract form (Hoover et al., 1999).

Received July 19, 2001; revised Oct. 12, 2001; accepted Nov. 9, 2001.

This work was supported by Ohio University, a Human Frontier Science Project Grant, National Science Foundation Grant 9309986, and National Institute of Mental Health Grant MH57832 to S.L.H. and an Ohio University Student Enhancement Award to N.J.H. We thank Ralph DiCaprio, Jeff Thuma, and Charles Geier for comments on this manuscript.

Correspondence should be addressed to Scott L. Hooper, Neuroscience Program, Department of Biological Sciences, Irvine Hall, Ohio University, Athens, OH 45701. E-mail: hooper@ohio.edu.

Copyright © 2002 Society for Neuroscience 0270-6474/02/221895-10\$15.00/0

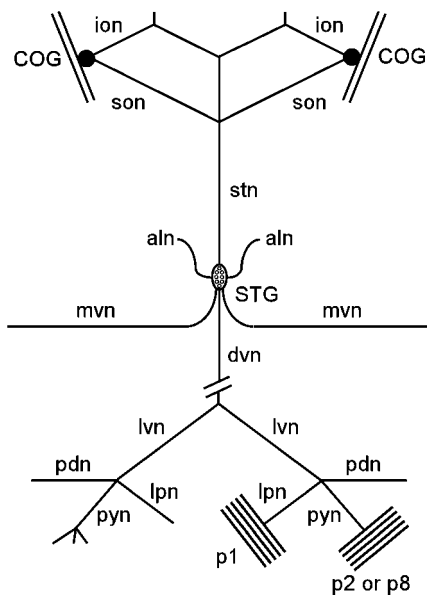


**Figure 1.** The stomatogastric nervous system and muscles p1, p2, and p8. The stomatogastric ganglion (STG) contains all pyloric motor neurons; their axons reach their muscles via the motor nerves of the system. Muscle p1 is innervated by the LP neuron, and muscles p2 and p8 are innervated by the PY neurons; the axons of the neurons reach the muscles via the dvn, lvn, and lpn or pyn. COG, Commissural ganglion; ion, inferior esophageal nerve; son, superior esophageal nerve; stn, stomatogastric nerve; aln, anterior lateral nerve; mvn, medial ventricular nerve; pdn, pyloric dilator nerve.

## MATERIALS AND METHODS

Spiny lobsters (500–1000 gm) were obtained from Don Tomlinson Commercial Fishing (San Diego, CA) and maintained in aquaria with chilled (13–15°C) circulating artificial seawater. Stomachs were dissected from the animals in the standard manner for muscle preparations (Selverston et al., 1976; Morris and Hooper, 1997; Harness, 1998). The p1, p2, and p8 muscles are bilaterally symmetrical muscle pairs that insert and attach to pyloric ossicles. A thin layer of connective tissue was carefully removed from the dorsal surface of muscles p1, p2, and p8 to allow intracellular muscle fiber recordings. In preparations in which muscle contraction was measured, one end of the muscle was carefully teased from its insertion or attachment and attached with a wire hook to a Harvard Apparatus (Holliston, MA) 60–3000 isotonic transducer. Transducer output was amplified 5- to 50-fold (depending on the muscle) by a Tektronix (Wilsonville, OR) AM502 differential amplifier. Muscle length and loading were adjusted for each muscle to achieve optimal contractions; muscle overstretching between trials was prevented by placing a bar under the far end of the transducer arm. Preparations were continuously superfused with chilled (12–15°C), oxygenated *Panulirus* saline with 40 mM glucose.

The p1 muscle is innervated by the lateral pyloric neuron, and the p2 and p8 muscles are innervated by the pyloric neurons (Maynard and Dando, 1974; Govind et al., 1975). The axons of both neuron types travel to the muscles through the dorsal ventricular (dvn), lateral ventricular (lvn), and lateral pyloric (lpn) or pyloric (pyn) nerves (Fig. 1). Contractions were induced by lvn stimulation after the dvn was cut to prevent spontaneous pyloric network activity from reaching the muscle. For the p2 and p8 muscles, which are innervated by multiple axons, stimulation amplitude was progressively increased until all axons were activated (despite the variation in EJP amplitude shown below, the stepwise increase in EJP amplitude with increasing stimulation voltage was apparent).

Nerve stimulations were performed using a World Precision Instruments (Sarasota, FL) stimulator and stimulus isolation unit and bipolar stainless steel pin electrodes insulated with petroleum jelly. Intracellular recordings were made with glass microelectrodes (filled with 0.55 M K<sub>2</sub>SO<sub>4</sub> and 0.02 M KCl, resistance 10–20 MΩ) and an Axoclamp 2A or 2B (Axon Instruments, Foster City, CA). Signals were recorded on a Microdata (South Plainfield, NJ) DT-800 digital tape recorder. EJP

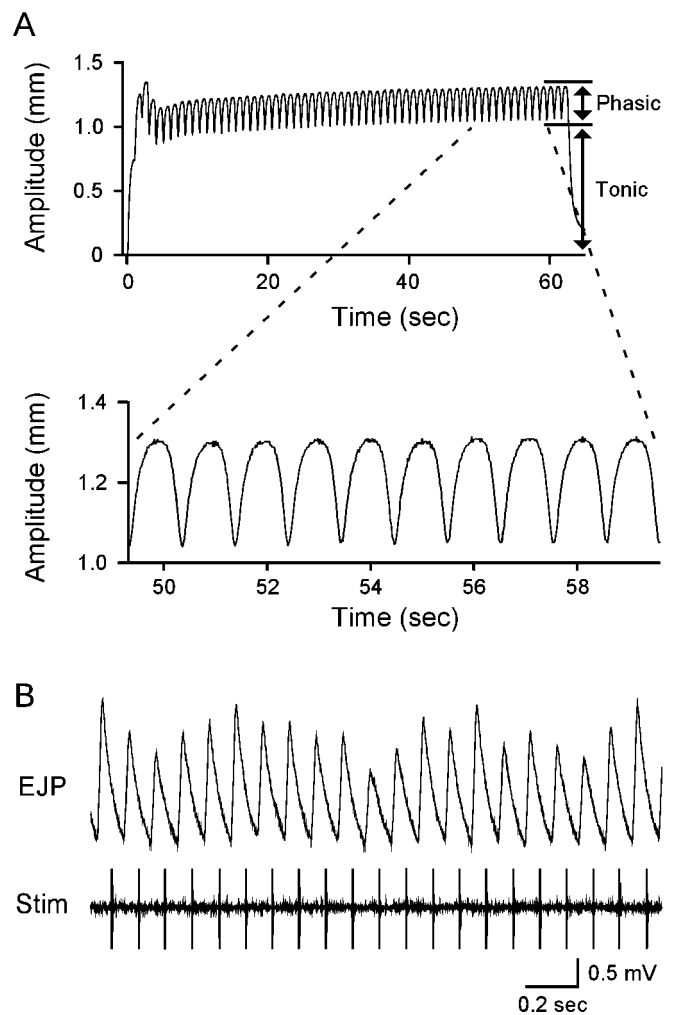


**Figure 2.** Electrical responses with a large-amplitude variation give rise to extremely regular muscle contractions. *A*, Stimulation of a p1 muscle with bursts of action potentials (20 Hz burst spike frequency, 0.2 sec burst duration, 5 spikes/burst) every second. The contractions temporally summate, and at steady state consist of a sustained baseline (Tonic) contraction on which ride phasic contractions in time with each stimulation burst. *Bottom panel* shows a time and amplitude expansion of a portion of the data in the *top panel*; note that the contraction amplitude shows very little variation (in this experiment, less than  $\pm 4\%$  of the mean). *B*, p1 muscle EJPs in response to tonic motor nerve stimulation at 10 Hz; EJP amplitudes show large-amplitude variations.

characteristics were measured using Spike II (Cambridge Electronics Design, Cambridge, UK) and Excel (Microsoft, Seattle, WA) and Kaleidagraph (Synergy Software) software after digitization by a Cambridge Electronics Design (Cambridge, UK) 1401plus. Statistics were calculated in Kaleidagraph (Synergy Software), and figures were prepared with Canvas (Deneba Software). The intracellular data presented here are from 18 preparations. The simulation shown in Figure 14 was performed in Neuron.

## RESULTS

Figure 2*A* shows an isotonic (constant tension) p1 muscle contraction induced by rhythmic motor nerve stimulation (1 Hz cycle period) with bursts of action potentials (20 Hz burst spike frequency, 0.2 sec burst duration, 5 spikes/burst). The top panel shows the complete 65 sec stimulation. Most pyloric muscles are very slow, and hence exhibit large intercontraction temporal summation. When the temporal summation stabilizes, the muscle contraction therefore consists of a large tonic baseline contraction

on which phasic contractions in phase with the burst stimulation ride (Morris and Hooper, 1998).

We are concerned here with the amplitude of the phasic contraction component. The bottom panel shows an expanded time and amplitude view of the phasic contractions after temporal summation had stabilized. The contractions show very little variation. Experimental noise limits our ability to measure this variation, but in this stimulation in the last 20 contractions the amplitude range was less than  $\pm 4\%$  of mean contraction amplitude. This extremely small variation in phasic contraction amplitude (after the temporal summation had stabilized) is a consistent feature of pyloric muscle contraction when the muscles are stimulated with bursts containing physiological numbers of action potentials (5–10; recordings from dozens to hundreds of muscles covering all major pyloric muscle groups including cpv1b, cpv2b, cv1, cv2, p1, p2, and p8; Ellis et al., 1996; Koehnle et al., 1997; Harness et al., 1998; Harness, 1998, Morris and Hooper, 1998, 2001). We have not performed a detailed analysis of the thousands of rhythmic muscle contraction sequences we have obtained, but in no cases was amplitude variation visually apparent with stimulations using bursts with physiological spike numbers. To confirm these visual observations, detailed analysis of the normalized phasic contraction amplitude variation in contraction sequences from seven p1 muscles stimulated with bursts containing 5–10 action potentials were made. The stimulations were continued until the tonic contraction amplitude had stabilized, and the amplitudes of 10–30 phasic contractions were measured. The smallest of these contractions was subtracted from the largest of them to determine the absolute contraction amplitude range, and this number was normalized by dividing by the mean contraction amplitude and multiplying by 100. This normalized range was expressed as a plus or minus around the mean by dividing by 2. In these p1 muscles normalized phasic contraction amplitude variation ranged from  $\pm 0.4$  to  $\pm 5.8\%$ , with an average variation of  $\pm 2.0$  (SD,  $\pm 1.8$ ).

We were therefore surprised to find that muscle fiber EJP amplitude showed large, visually apparent variations. Figure 2*B* shows intracellular recordings of EJPs in a p1 muscle fiber in response to tonic, 10 Hz motor nerve stimulation; EJP amplitude shows an almost twofold variation. The question we investigated was how muscle electrical responses with such large variability gave rise to muscle contractions with so little. One immediate explanation could be that the muscles were being driven close to the maximum contraction they can produce, and this saturation limited the variability of the contractions. However, small variability continued to be present when the muscles were driven with stimulations that induced far from maximal contractions (the contraction in Fig. 2*A* was less than half of the maximum contraction this muscle could produce, and those used in the average above were similarly from stimulations that induced contraction amplitudes far from the maximum contraction the muscle can produce).

### Tonic stimulations

We first determined the average and range of EJP amplitudes for the p1 muscle and two other intrinsic pyloric muscles, p2 and p8, to tonic motor nerve stimulation (Fig. 3). The top panel shows unnormalized data from six p1, five p2, and four p8 muscles fibers. For each muscle, these data were obtained from at least three different preparations. In all cases at least 1 min of stimulation (600 EJPs) was performed, and, although no obvious facilitation was seen, data were not taken for the first 10–15 sec. The bars

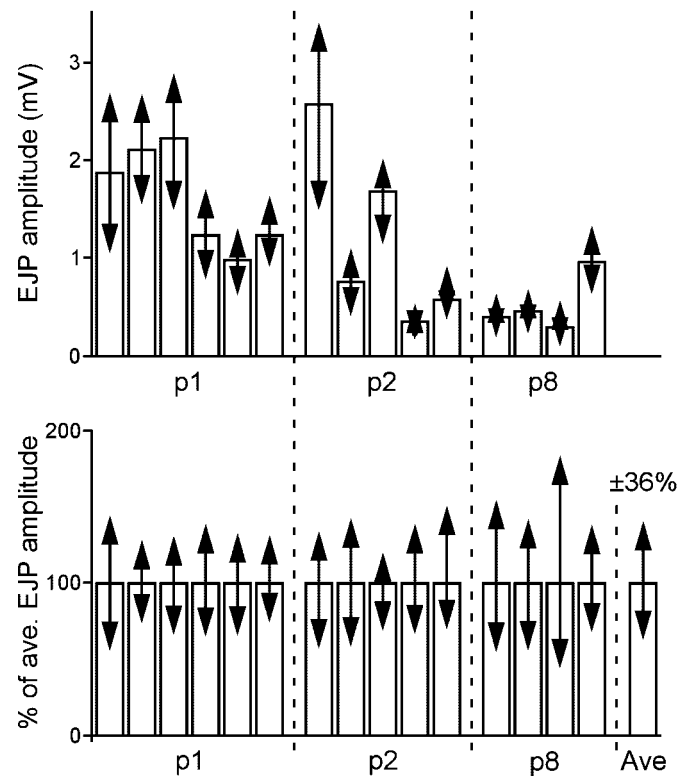


**Figure 3.** Summary plot showing EJP amplitude variation for several p1, p2, and p8 muscles. *Top plot* shows variation as a function of amplitude. Each bar shows average EJP amplitude for one muscle fiber; the arrows show the range of EJP amplitudes observed in the fiber. The variation range scales with average EJP amplitude. *Bottom plot* shows same data normalized to average EJP amplitude; all muscle fibers show similar normalized EJP amplitude ranges. Last bar (labeled *Ave*) shows that the average normalized EJP amplitude range is  $\pm 36\%$  of the mean.

show average EJP amplitude for each fiber; the arrows show the entire range of EJP amplitudes present in the data set. All the muscle fibers and muscles show EJP amplitude variation, but the variation scales with average EJP amplitude. We therefore normalized the data to average EJP amplitude (bottom panel); in all cases the relative EJP amplitude range is similar. The last bar (labeled “Ave”) in the bottom panel shows that the average normalized range (across all three muscles) was  $\pm 36\%$  of mean EJP amplitude.

This large-amplitude range variation could arise from a few outliers in a data set in which the points are otherwise clustered very near the mean. We therefore binned the data by EJP amplitude and plotted the percentage of total EJPs present in each bin. Figure 4 shows representative data for fibers from each muscle. Although there is a peak around the mean value, it is quite broad—the maximum percentage in any one bin is 18%, and for each muscle, bins containing  $\geq 5\%$  of the total points span  $\sim 50\%$  of the range. Similar broad peaks were seen in all muscle fibers studied, and thus the EJP amplitude variability is not caused by scattered outliers.

Another source of regularity that could reduce muscle contraction variability would be a repeating pattern of EJP amplitude variation. To test this possibility, we plotted the amplitude of each EJP versus the amplitude of the EJP that preceded it (Fig. 5) to see if any pattern was revealed. For instance, if each small EJP was followed by a large EJP and vice versa, this plot would show a line with a negative slope. The points instead form a cloud, and

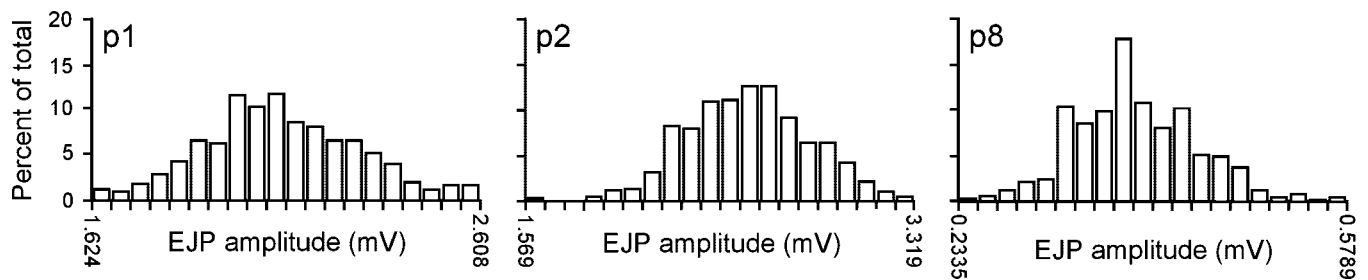


**Figure 4.** EJP amplitude variation is not caused by a few scattered outliers. The three panels show binned data from one fiber in a p1 (left), p2 (middle), and p8 (right) muscle. Although the amplitude distributions are peaked, the peaks are quite broad, and for each muscle bins containing  $\geq 5\%$  of the total points span  $\sim 50\%$  of the range.

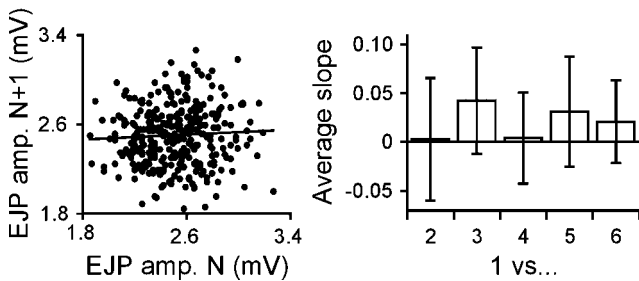


**Figure 5.** There is no long-term pattern to the EJP amplitude variation. *Left*, Plot of the amplitude of each EJP versus the amplitude of the EJP that preceded it; no dependence of present EJP amplitude on preceding EJP amplitude is apparent. *Right*, Average slopes of EJP amplitude versus the amplitude of the second, third, fourth, fifth, and sixth EJPs before it; in no cases was a linear dependence, or any pattern in the data, observed.

linear regression of the data has a slope near zero. Similar analyses were performed in which the amplitude of each EJP was plotted versus the second EJP before it, the third before it, etc. up to the sixth before it. In no case in any of the muscles was any pattern apparent, and all linear regressions had slopes that were not significantly different from zero ( $\alpha = 0.05$ ; Student's *t* test, unequal variances assumed, right panel). The data in Figures 3–5 thus indicate that the EJP variation shown in Figure 2*B* is present in all muscle fibers of the three pyloric muscles, that this variation is not caused by rare outliers and that no apparent regularity exists in the ordering of the differently sized EJPs.

### Burst stimulations

Both the muscle contractions shown in Figure 2*A*, and contractions *in vivo*, are driven by bursts of spikes. It was thus possible that if the muscles were stimulated with spike bursts, the EJP amplitude variation would be reduced or abolished. For instance, if in the tonic stimulations the EJPs were facilitated, it was possible that, in a burst stimulation paradigm, facilitation would decay during the interburst intervals and increase during the burst. If the amount of facilitation was larger than the EJP amplitude variability, then all first EJPs would be smaller than all second EJPs, and all second EJPs smaller than all third EJPs, and thus relative variability would decrease. To examine this issue, we stimulated the muscles with 3-spike bursts (we were unable to successfully hold the electrode recordings throughout the experiments with bursts containing larger spike numbers). Figure 6*A* shows raw data for a p1 muscle fiber stimulated with 3-spike bursts (interburst spike frequency, 10 Hz) every 1 sec (the average cycle period of the input this muscle physiologically receives). For the second and third spikes in the burst, we measured amplitude from the beginning amplitude of the EJP on the declining phase

of the previous EJP (dashed lines, last burst). Figure 6*B* shows the amplitudes of the first, second, and third EJPs in each burst for 60 bursts and Figure 6*C* shows the average and range of the first, second, and third EJPs for several muscle fibers from p1, p2, and p8 (again, these data are from at least three preparations for each muscle). Each column triplet is data from one muscle fiber; the first column in the triplet is data from the first EJPs, the second data from the second EJPs, and the third data from the third EJPs. Figure 6*D* shows normalized data. When the muscle is stimulated in bursts, EJP amplitude variation is only slightly less than that seen in tonic stimulations ( $\pm 33\%$  for burst stimulation,  $\pm 36\%$  for tonic stimulation).

This analysis shows that consistent changes in EJP amplitude do not occur as a function of what number a given spike is in the burst. However, it does not address other possible regularizing influences that are possible in burst stimulation, in particular combinatorial averaging. Even if individual EJP amplitude is stochastic, it is still more unlikely for a burst to have three small or large EJPs than to have a mixture of small and large EJPs. Therefore, if EJP amplitudes were added, combinatorial averaging would make the summed EJP amplitude distributions more sharply peaked than were the single EJP distributions. Note that this would not decrease the normalized range—bursts with all small and all large EJPs would still occur—but it is possible that they could become sufficiently rare that their functional significance was small, particularly in bursts with large spike numbers. This is a particularly important issue because the muscles being studied are graded and contract very slowly (Ellis et al., 1996; Harness et al., 1998) (M. Rehn, L. Morris, and S. Hooper, unpublished observations), and thus do not contract in response to each EJP, but instead to the total number of EJPs in the burst (Morris and Hooper, 1997; Harness, 1998; Harness et al., 1998), and because these muscles can receive as many as 10–12 spikes per burst.

We examined this issue in three ways. Our first effort was to compare the relative variation (amplitude variation divided by average contraction amplitude) in contraction amplitude in muscles stimulated with 3-spike bursts (the muscles do not contract when stimulated with bursts containing  $\leq 2$  spikes) with that observed in muscles stimulated with multiple ( $> 5$ ) spike bursts, in which combinatorial averaging would be pronounced. Figure 7*A* shows p1 muscle contraction with 10 spikes/burst, and Figure 7*B* shows contraction in the same muscle fiber with 3 spikes/burst. To show the relative variation in contraction size, the amplitude calibrations (vertical axes) in the two figures have been adjusted so that the contractions in each panel have the same apparent size. Consistent with combinatorial averaging, the relative variation in the three-spike case is much larger than in the multispike case. Figure 7, *C1* and *C2*, shows a comparison of the largest and

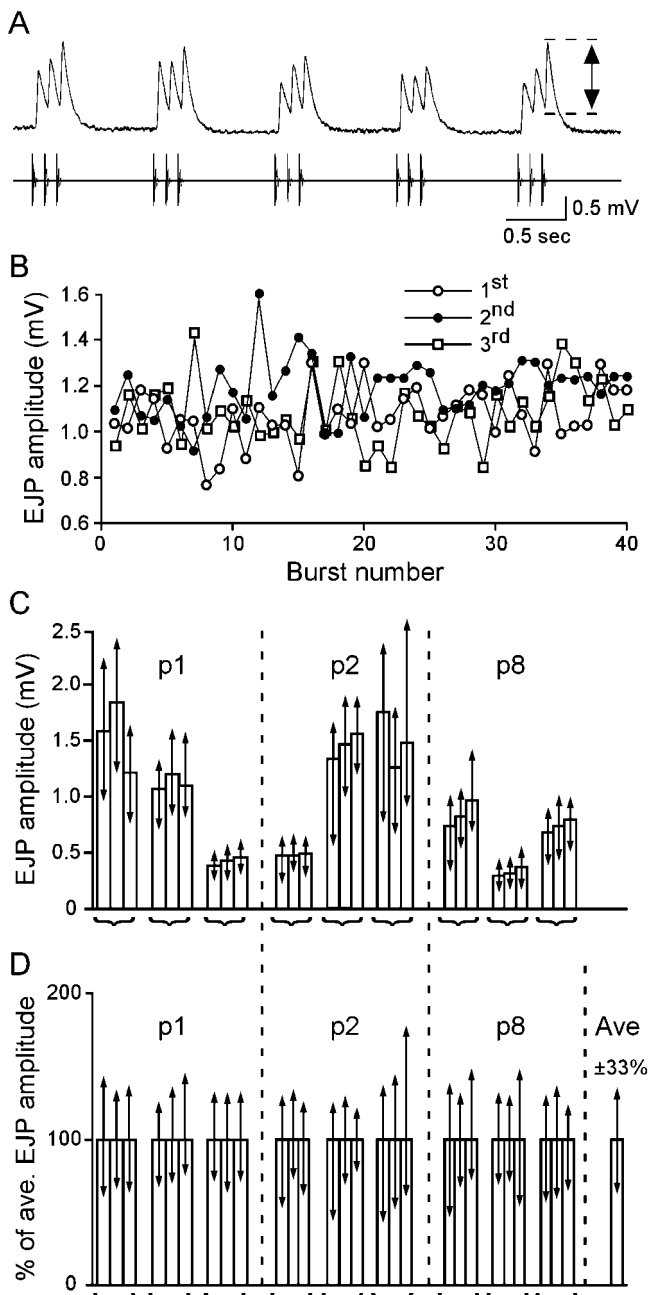


**Figure 6.** EJP amplitude continues to show large variation when the muscle is stimulated with bursts. *A*, p1 muscle EJPs in response to 3-spike burst stimulation (interburst spike frequency, 10 Hz) every 1 sec. *B*, EJP amplitude induced by the 1st, 2nd, and 3rd spike each burst; no pattern or facilitation is apparent. *C*, p1, p2, and p8 mean EJP amplitude (bars) and range (arrows) of the EJPs induced by the 1st, 2nd, and 3rd spikes (each set of three bars is from one fiber; the 1st bar is the 1st EJP, the 2nd bar is the 2nd EJP, the 3rd bar is the 3rd EJP). *D*, Data normalized to mean EJP amplitude; bar marked *Ave* is the average of all data. Average normalized range is  $\pm 33\%$  of the mean.

smallest muscle contractions in Figure 7, *A* and *B* (the same scales are used in *7C1* and *7C2* as in *7A* and *7B*, respectively); the relative variation in Figures *7A* and *C1* is only  $\pm 0.4\%$ , whereas that in Figure *7B* and *C2* is  $\pm 14\%$ . This is an extreme example, but in each of seven p1 muscles in which 3- and many-spike bursts were compared, relative contraction amplitude variation decreased with high burst spike number (three-spike mean variation  $\pm 12.8 \pm 7.6\%$  (SD); multi-spike,  $\pm 2.0 \pm 1.8\%$ ).

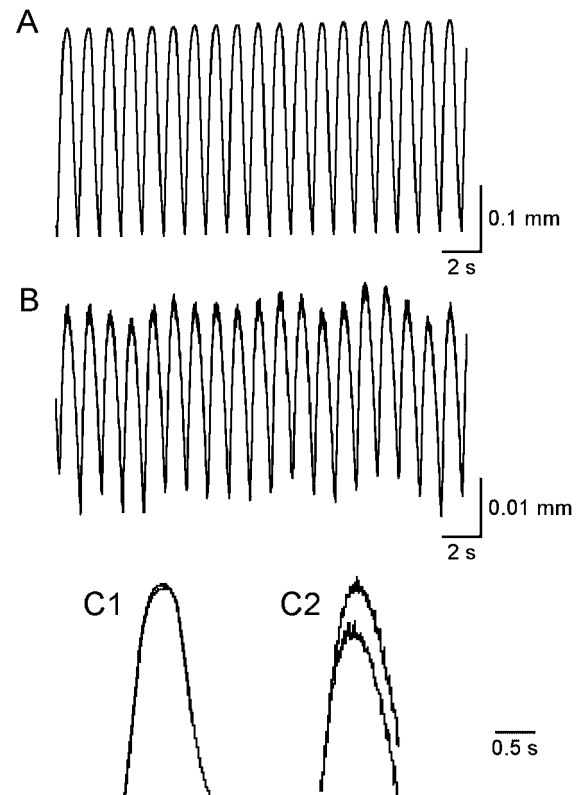


**Figure 7.** Relative variation in contraction amplitude decreases as burst spike number increases. *A*, p1 muscle contractions in response to 10-spike bursts delivered every 1 sec. *B*, Contractions of the same muscle in response to 3-spike bursts delivered every 1 sec. Note that the amplitude calibrations (vertical axes) in the two panels have been adjusted so that the contractions in the two panels appear to have the same average amplitude. *C1*, *C2*, Comparison of the largest and smallest contractions in *A* and *B*; the same amplitude scales are used in *C1* and *A* and in *C2* and *B*.

We next turned to examining the effect of combinatorial averaging on EJP summation in multispike stimulations. Before addressing this issue, however, it is important to consider what is the best measure of muscle electrical excitation in burst stimulation. In the single spike stimulation protocols, and in the analysis of individual EJPs in a burst presented above, EJP amplitude was used as a measure of muscle excitation. The EJPs in our muscles decline exponentially and (in a single muscle) with an approximately constant time constant regardless of summated depolarization amplitude. In this case EJP area

$$A = \int_0^{\infty} a e^{-t/\tau} dt = -a\tau e^{-t/\tau} \Big|_0^{\infty} = a\tau,$$

where  $a$  is EJP amplitude. For single spike EJPs amplitude and area are therefore linearly proportional, and hence are equivalent measures of muscle excitation.

In burst stimulations, however, compound EJP amplitude (the maximum amplitude achieved within the temporally summated EJPs) and compound EJP area (the area underneath the temporally summated EJPs) are not linearly related. For instance, two very closely spaced spikes would result in a summated EJP with an amplitude approximately equal to the sum of the individual EJP amplitudes, whereas two widely spaced spikes would result in a much lower compound EJP amplitude because the second spike

would fall far into the decline of the first EJP. However, we show in the appendix that in each case the compound EJP area is the same. As such, for burst stimulations we have a choice as to whether to use compound EJP amplitude or compound EJP area as the measure of muscle excitation.

Little is known on the molecular level about excitation–contraction coupling in pyloric muscles, and this decision therefore cannot be made on this basis. However, studies investigating whether, for physiologically relevant burst spike numbers, burst spike number or intraburst spike frequency primarily determines muscle contraction amplitude suggest that compound EJP area is the more important parameter functionally. The depolarizations physiologically relevant spike bursts induce in these muscles are far from the synaptic reversal potential ( $\sim 0$  mV; Lingle, 1980), and thus higher spike frequency should induce a greater compound EJP amplitude. If compound EJP amplitude primarily determined muscle contraction, contraction would therefore depend, at least in part, on spike frequency. However, in most pyloric muscles, contraction amplitude instead depends on burst spike number, regardless of the frequency with which the spikes are delivered (Morris and Hooper, 1997; Harness, 1998). Compound EJP area, but not compound EJP amplitude, similarly depends only on burst spike number. Furthermore, contraction amplitude in the graded accessory radula closer muscle in *Aplysia* is a linear function of compound EJP area, not amplitude (Cohen et al., 1978). For these two reasons we chose to examine compound EJP area in our analysis of burst stimulations.

We made a theoretical estimate of the effect of combinatorial averaging by using the single EJP amplitude probability distribution of a p1 muscle fiber (Fig. 4, first panel) to calculate the probability distribution of summed EJP area for 3-, 5-, 6-, and 7-spike bursts (Fig. 8; see legend for details). We defined the summed EJP area distribution range as all probabilities  $>2\%$ . As expected, the range decreased as burst spike number increased, and was reduced  $\sim 25\%$  for 3-spike bursts, and  $\sim 50\%$  for 7-spike bursts. However, the regularizing effect of combinatorial averaging decreased as spike number increased (compare 5-, 6-, and 7-spike cases), and hence this mechanism alone cannot explain the at least 10-fold decrease in variation seen in comparing tonic EJP amplitude to muscle contraction amplitude.

We examined this issue experimentally by measuring the variation in compound EJP area in burst stimulations for three p1, three p2, and two p8 muscle fibers (Fig. 9A shows raw data, and Fig. 9B shows normalized data; the data are from three different preparations for p1 and p2, and two for p8). The average range is only  $\pm 11\%$ , one-third of the  $\pm 33\%$  amplitude variation in the EJPs responsible for the summation (Fig. 6, “Ave” column). This is considerably larger than the 25% reduction for three spikes shown in Figure 8, but range diminution caused by combinatorial averaging is a function of how broad the one-spike range is, and the probability level used to define the diminution. For instance, if the 1-spike data were more flat and a 5% probability level was used, a threefold range diminution could be easily obtained. The data shown in Figures 8 and 9 thus indicate that in burst stimulation combinatorial averaging should result in a twofold to threefold reduction of the variation observed in tonic stimulations.

### Intramuscle and intermuscle fiber averaging

When pyloric muscle length constant ( $\lambda$ ) is measured by penetrating a muscle fiber with two distantly spaced electrodes, injecting current into one and measuring the induced voltage change in the other, and sequentially repeating this procedure as the voltage

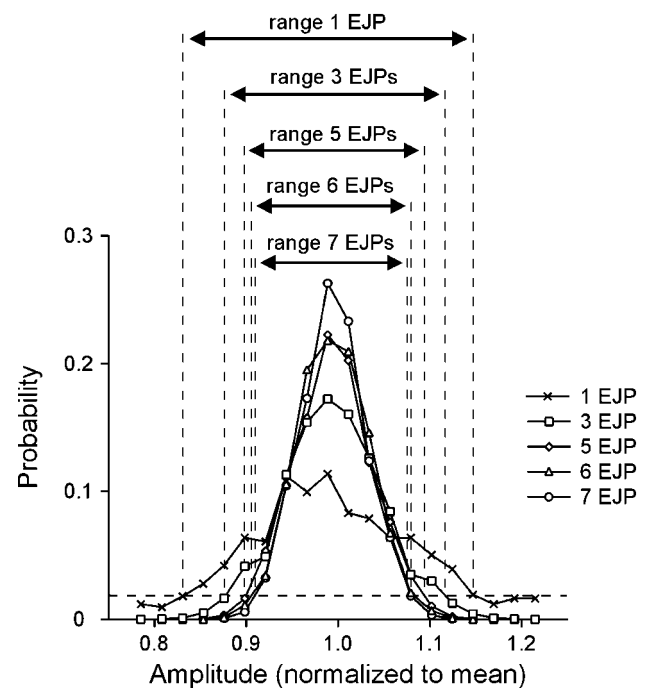


**Figure 8.** Combinatorial averaging reduces effective range, but only to a limit. The data in the p1 panel in Figure 4 was used to calculate the probability distribution of the summed EJP amplitude that 3-, 5-, 6-, and 7-spike bursts would induce. If a 2% probability is taken as the effective range (horizontal dashed line), combinatorial averaging results in a 25% reduction in range with 3-spike bursts and a 50% reduction with 7-spike bursts. However, the range diminishing effects of combinatorial averaging rapidly decrease as burst spike number is further increased (compare 5-, 6-, and 7-spike ranges). The data shown in this figure were calculated as follows. First, the EJP amplitudes in the 20 bins of the single spike distribution were added in all possible combinations. For instance, for the two spike case, the amplitude of bin 1 was added to the amplitudes of bins 1 to 20, the amplitude of bin 2 was added to the amplitudes of bins 1 to 20, the amplitude of bin 3 was added to the amplitudes of bins 1 to 20, etc. to obtain all amplitudes that could result from summing the EJPs induced by two spikes. Second, each summed amplitude was assigned a probability by multiplying the probabilities of the single spike probabilities that gave rise to it. Third, the summed EJP amplitudes were normalized to the mean summed EJP amplitude and binned (20 bins) according to normalized summed EJP amplitude. The probabilities of the normalized summed EJP amplitudes in each bin were then summed to calculate the probability of that bin's amplitude occurring. Computational limitations prevented us from performing this analysis for spike bursts containing  $>7$  spikes, but the reduction in variation with increasing spike number (compare the 5-, 6-, and 7-spike traces) suggests that little further reduction would occur in higher spike number bursts.

measuring electrode is moved closer to the current injecting electrode,  $\lambda$  is 1.5–2 mm (E. Marder, personal communication). We have confirmed this measurement by similar multielectrode measurements. (A possible criticism of this technique is that muscle fiber resistance could be decreased by the multiple electrode impalements, which might lead one to believe that, because  $\lambda$  is proportional to the square root of membrane resistance, these measurements were underestimating the true length constant. However, we show in the Appendix that, because the damage is localized to distal regions of the fiber, such damage actually results in an overestimation of  $\lambda$  and that the error so induced is likely to be small.)

Since the p1, p2, and p8 muscles are  $\sim 10$  mm long (Maynard and Dando, 1974), they thus contain several length constants. These data suggest that the EJPs we were measuring were a local phe-

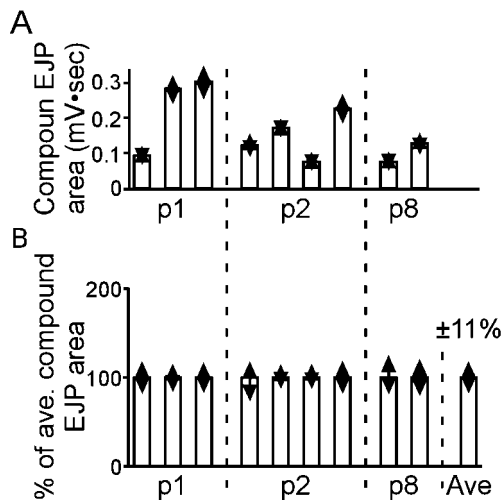


**Figure 9.** Compound EJP area shows a considerable reduction in variability. *A*, Mean (bars) and range of compound EJP area of p1, p2, and p8 muscle fibers. *B*, Data normalized to mean compound EJP area; the average variation (bar marked "Ave") is only  $\pm 11\%$ . See Results for discussion of difference in variation reduction between this figure and Figs. 6 and 8.

nomenon, that EJPs measured at distant locations in a single muscle fiber would be uncorrelated, and intrafiber averaging of EJP amplitude would thus occur and help regularize muscle contraction. To test this possibility we recorded simultaneously from well separated (5–8 mm apart) locations in single muscle fibers and plotted EJP amplitude at one site against EJP amplitude at the other (Fig. 10). Surprisingly, in all three muscles EJP amplitudes were highly correlated at all recording sites. The source of this unexpected correlation is unclear (see Discussion), but these data do indicate that intrafiber averaging is unlikely to explain why muscle contraction shows such small variation. When summed EJP amplitude or compound EJP area was measured, they were similarly highly correlated within single fibers (data not shown).

An additional source of variation reduction would be if the EJPs in different muscle fibers were uncorrelated, because the EJP amplitude variation in individual fibers would be averaged across all the fibers of the muscle. Figures 11 and 12 show that this intermuscle fiber averaging occurs. Figure 11*A* shows raw recordings from two p1 muscle fibers in response to tonic motor nerve stimulation; the EJP amplitude variations of the two fibers do not appear correlated. This lack of correlation was quantified by plotting the EJP amplitude of one fiber in the muscle versus the amplitude of another; Figure 11*B* shows these plots for fibers from muscle p1, p2, and p8. The data points form a cloud, and linear regressions to the data are near horizontal with  $R^2$  near zero. Similar lack of correlation between different muscle fibers was seen when summed EJP amplitude for 3-spike burst stimulations was compared (data not shown). Surprisingly, however, when compound EJP areas in different muscle fibers were measured, a range of correlations, some strong, were observed. Figure 12 shows  $R^2$  values of linear regressions of compound EJP area between muscle fibers for p1, p2, and p8 muscles; regression coefficients range from near 0 to almost 0.8. Given the lack of correlation of single or summed EJP amplitudes, the basis of the high correlations for compound EJP area between some muscle fibers is unclear. However, in all three muscles some fibers were uncorrelated by all measures, and thus interfiber averaging is likely also to contribute to regularization of muscle contraction amplitude.

## DISCUSSION

We investigated the mechanisms that transform muscle electrical responses with a large-amplitude variation to highly deterministic muscle contractions. This transformation does not arise because of the variation arising from only a few outliers (Fig. 4), long time scale regularity (Fig. 5), burst stimulation decreasing EJP amplitude variation (Fig. 6), or intramuscle fiber averaging (Fig. 10). This transformation instead appears to result from combinatorial averaging in individual muscle fibers of the different sized EJPs in burst input (Figs. 8, 9) and averaging across muscle fibers with uncorrelated electrical responses (Figs. 11, 12).

### Comparison to earlier work on stomatogastric muscle EJPs

Sen et al. (1996) describe a generally applicable fitting procedure that allows postsynaptic response to be predicted from any pre-synaptic input. When tested on the electrical responses of two gastric mill muscles in the crab *Cancer borealis*, the procedure resulted in predictions with a 10–20% normalized error. Given the large EJP amplitude variation reported here, it may seem that our data and the data of Sen et al. (1996) contradict. However, the muscles Sen et al. (1996) used show large EJP facilitation. In muscles whose EJP amplitudes show large variation, if EJP facilitation is much larger than the range of the variation, much of the electrical response will nonetheless be predictable. It is thus likely that their data and our data agree; the Sen et al. (1996) procedure accurately captured the synaptic facilitation and depression of the system, and the remaining error arose from inherent EJP amplitude variation similar to that described here. This interpretation is supported by examination of Figures 6 and 8 of Sen et al. (1996), which show EJP amplitude variation in tonic stimulation trains in which facilitation has largely stabilized.

### Implications for pyloric function

The variation of EJP amplitude and area make it unlikely that fine variations in spike timing within motor neuron bursts will affect muscle contraction, because even if some facilitation and/or depression occurs at these synapses, our data suggest that the inherent variation overwhelms this regularizing influence. This observation is consistent with work on these muscles showing that burst spike number, not spike frequency, codes phasic contraction amplitude (Ellis et al., 1996; Morris and Hooper, 1997; Harness, 1998; Harness et al., 1998) (Rehn, Morris, and Hooper, unpublished observations).

### What gives rise to the EJP amplitude variability?

Pyloric motor neurons synapse at multiple sites along pyloric muscle fibers (Atwood et al., 1977, 1978; Atwood and Wojtowicz, 1986). *A priori*, two explanations for the EJP amplitude variability reported here thus exist. One is that the muscle fibers are essentially isopotential (fiber length less than two length constants) and the variability arises from variability in vesicle number released at each synaptic site during each spike. Given the large number of synaptic sites and large variation in quantal number observed at some crustacean synapses (Atwood and Wojtowicz, 1986), this variation would give rise to the smooth variation in EJP amplitude we observe. However, the short  $\lambda$  measured with multiple penetrations contradicts this explanation, because these data imply that the muscle fiber is not isopotential, and hence different synaptic sites are electrically isolated from each other. Pyloric muscle diameter is such that relatively small changes in membrane resistance would induce large length constant changes (Appendix), and thus the faint possibility exists that some exper-

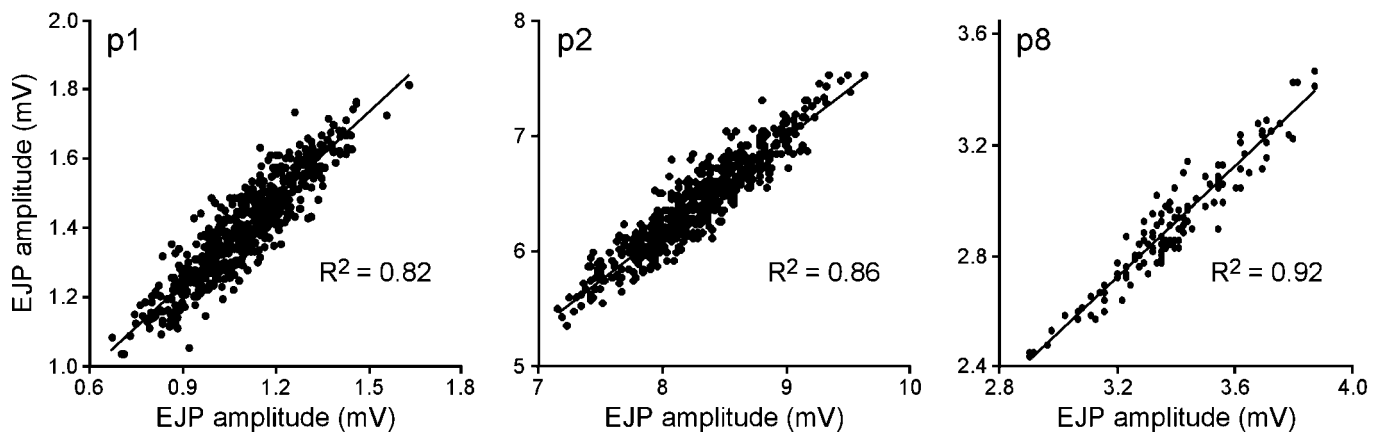


**Figure 10.** Averaging of different-sized EJPs at different locations within a single fiber does not explain constant amplitude muscle contractions. Two electrodes were placed in single muscle fibers at sites 5–8 mm apart, and the EJP amplitudes recorded at one site were plotted against those recorded at the other. In all muscles EJP amplitudes at both sites were well correlated.

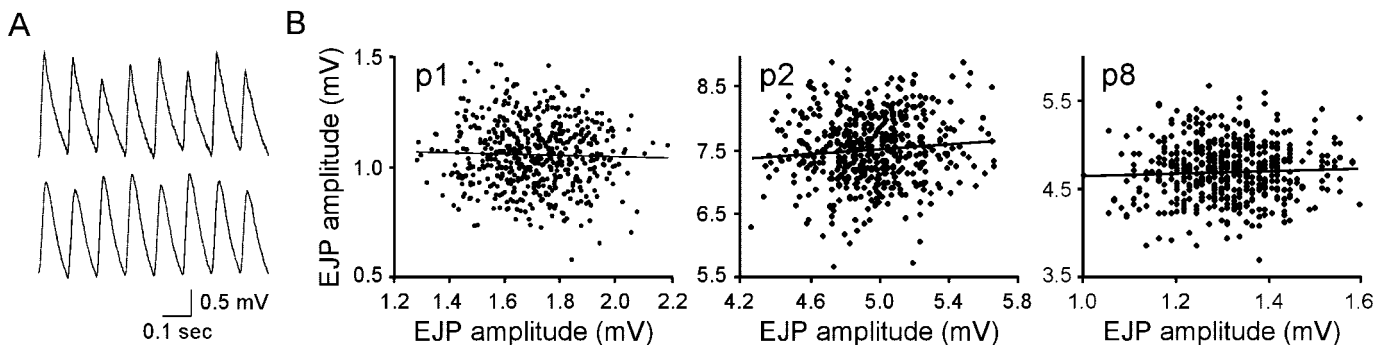


**Figure 11.** Averaging of uncorrelated EJP amplitudes across muscle fibers contributes to constant amplitude muscle contractions. *A*, Recordings from two p1 muscle fibers. Amplitude variations do not appear to be correlated. *B*, Plots of EJP amplitude in one muscle fiber versus EJP amplitudes in a second for a p1 (top), p2 (middle), and p8 (bottom) muscle. In no cases is any correlation apparent. The vertical “columns” in p8 data are quantization artifacts that occurred in data digitization.

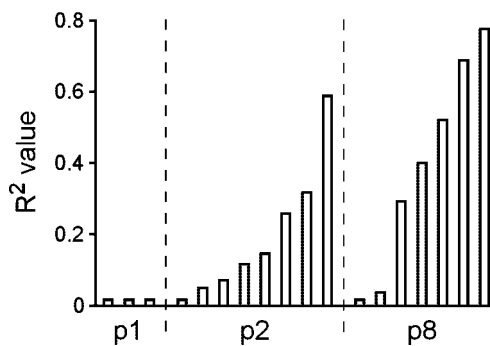


**Figure 12.** Compound EJP area shows a range of correlation between different muscle fibers. Plots of the  $R^2$  value of linear regressions to data similar to that shown in Figure 10*B*, but to compound EJP area instead of EJP amplitude. A range of  $R^2$  values from near 0 to almost 0.8 is observed. However, in all muscles some fibers are uncorrelated, and so cross-fiber averaging presumably helps regularize muscle contraction.

imental perturbation associated with repeated impalements is decreasing muscle length constant (as shown in the Appendix, localized damage by multiple electrode penetration would not have this effect). However, why this decrease would occur in experiments in which muscle length constant was measured, but not when dual electrode recording was used to measure EJP variability, is unclear. One possibility would be that tonic nerve

stimulation increases muscle input resistance, which would increase muscle length constant. However, experiments in two p1 muscles showed that tonic nerve stimulation does not alter muscle input resistance significantly.

The second explanation is that multiple axons, or multiple branches of a single axon, innervate the muscles, and the variability arises from spike conduction failure in either individual axons or branches of a single axon. This explanation requires that each axon or branch make synaptic contacts along the whole length of the muscle fiber, because otherwise spike conduction failure would affect only a region of the fiber, which is inconsistent with the high correlation in different regions we observe. Methylene blue staining shows that the nerves innervating these muscles often do branch at the muscle, but we are unable to follow these very small branches to ascertain if they course along a substantial portion of its length. If the number of such branches were small, EJP amplitudes would be expected to vary in a stepwise manner because one or more branches failed. However, such stepwise variation was never observed (data not shown), which implies that relatively large numbers (more than five) of axons or branches innervate each fiber along its length. In *Panulirus* the p2 and p8 muscle fibers can be innervated by up to five axons (Govind et al., 1975), and thus, particularly if these axons branch in the muscle, spike conduction failure could easily explain our data. The p1 muscle, however, is innervated by only one axon, and this explanation would thus require that this axon branch

extensively and that each muscle fiber was innervated along its entire length by many of these branches. Although considerable work has been performed examining pyloric nerve–muscle synapse anatomy (Maynard and Dando, 1974; Govind et al., 1975; Atwood et al., 1978), we have been unable to locate work detailing the branching patterns of pyloric motor nerves within the muscles. *A priori*, such a complicated innervation pattern is difficult to accept, and so for this muscle, although the EJP correlation in individual fibers is clear, the source of the EJP variation is without adequate explanation.

### Comparison to other neuromuscular systems

The EJP variability reported here is not unique. The p1 muscle of the crab *Callinectes sapidus* and the opener muscle of the crayfish *Procambarus clarkii* show similar, apparently stochastic, EJP amplitude variations (Govind et al., 1975; Atwood et al., 1975), and excitatory junctional current area of crayfish extensor and shore crab (*Pachygrapsus*) opener muscles show variations of  $\pm 25$ –50% (Atwood and Wojtowicz, 1986; Msghina et al., 1998, 1999), all in response to tonic motor nerve stimulation. However, the difficulties these variations would pose for producing deterministic muscle contractions were not commented on in this work, and we have been unable to find previous work in which this apparent difficulty has been investigated.

In systems with spiking muscles, even if EJP amplitude did vary, this variation is unlikely to be important functionally, because once the muscle reaches threshold the active response of the muscle, not the size of its input, determines its twitch, and in most such systems the safety factor is large (EJP amplitude is considerably above spike threshold). However, a variety of lower vertebrate and invertebrate muscles, like pyloric muscles, are graded and nonspiking (Hoyle, 1953, 1983; Atwood and Hoyle, 1965; Hetherington and Lombard, 1983; Carrier, 1989), and for these muscles EJP reliability has important functional consequences. In most of these systems the motor neurons fire bursts of spikes, and so the same transformation of an electrical response with a large stochastic component into deterministic contractions could occur. Nonetheless, in light of the data reported here it would seem important to check EJP reliability in systems with graded muscles both to correctly describe the motor neuron to contraction relation, and to know the extent to which EJP amplitude can be deterministically predicted from motor neuron activity. With respect to muscle contraction, for both spiking and graded muscles the additional predictability afforded by cross fiber averaging reported here is, of course, a further mechanism by which muscle contraction can be made deterministic.

### Broader implications

Particularly at central synapses, synaptic release in response to single spikes shows large variability (Allen and Stevens, 1994; Stevens and Wang, 1995; Huang and Stevens, 1997; Simmons, 2000). Firing of multiple spikes by single presynaptic neurons or synchronous arrival of spikes from multiple presynaptic neurons results in more deterministic postsynaptic responses because of, respectively, synaptic facilitation and temporal summation in the dendritic tree (Borst and Egelhaaf, 1994; Stevens and Wang, 1995; Lisman, 1997; Stevens and Zador, 1998; Sherman, 2001; Swadlow and Gusev, 2001). The EJPs described here do not appear to appreciably facilitate, and this method of increasing synaptic fidelity is thus not present in these muscles. However, even without facilitation, the decrease in variation caused by bursting input that we describe here would presumably also occur

at neuron-to-neuron synapses. Similarly, the decreased importance of variation at each of two synapses when they are simultaneously active (presumably as a result of combinatorial averaging and temporal summation in the dendritic tree) is analogous to the effects of cross-fiber averaging reported here. Our data thus constitute a lower bound (because of the absence of facilitation) of the effectiveness of bursting input and postsynaptic averaging to produce deterministic postsynaptic responses from synapses with high inherent variability. The at least 10-fold reduction in variation we report here is striking evidence of how powerful these processes can be.

### REFERENCES

- Allen C, Stevens CF (1994) An evaluation of causes for unreliability of synaptic transmission. *Proc Natl Acad Sci USA* 91:10380–10383.
- Anderson JS, Lampl I, Gillespie DC, Ferster D (2000) The contribution of noise to contrast invariance of orientation tuning in cat visual cortex. *Science* 290:1968–1972.
- Atwood HL, Hoyle G (1965) A further study of the paradox phenomenon of crustacean muscle. *J Physiol (Lond)* 181:225–235.
- Atwood HL, Wojtowicz JM (1986) Short-term and long-term plasticity and physiological differentiation of crustacean motor synapses. *Int Rev Neurobiol* 28:275–362.
- Atwood HL, Swenarchuk LE, Gruenwald CR (1975) Long-term synaptic facilitation during sodium accumulation in nerve terminals. *Brain Res* 100:198–204.
- Atwood HL, Govind CK, Jahromi SS (1977) Excitatory synapses of blue crab gastric mill muscles. *Cell Tiss Res* 177:145–158.
- Atwood HL, Govind CK, Kwan I (1978) Nonhomogeneous excitatory synapses of a crab stomach muscle. *J Neurobiol* 9:17–28.
- Borst A, Egelhaaf M (1994) Dendritic processing of synaptic information by sensory interneurons. *Trends Neurosci* 17:257–263.
- Carrier DR (1989) Ventilatory action of the hypaxial muscles of the lizard *Iguana iguana*: a function of slow muscle. *J Exp Biol* 143:435–457.
- Cohen JL, Weiss KR, Kupfermann I (1978) Motor control of buccal muscles in *Aplysia*. *J Neurophysiol* 41:157–180.
- Douglass JK, Wilkens L, Pantazelou E, Moss F (1993) Noise enhancement of information-transfer in crayfish mechanoreceptors by stochastic resonance. *Nature* 365:337–340.
- Ellis TA, Donath AS, Morris LG, Thuma JB, Hooper SL (1996) Motor pattern expression of a lateral pyloric constrictor muscle. *Soc Neurosci Abstr* 22:131.
- Govind CK, Atwood HL, Maynard DM (1975) Innervation and neuromuscular physiology of intrinsic foregut muscles in the blue crab and spiny lobster. *J Comp Physiol* 96:185–204.
- Harness PI (1998) Prediction of spiny lobster stomatogastric muscle contractions in response to physiologically relevant, constant duty cycle rhythmic neural input, Senior thesis, Ohio University Honors Tutorial College.
- Harness PI, Morris LG, Hooper SL (1998) Intrinsic pyloric muscle output predicted from constant duty cycle rhythmic neural input. *Soc Neurosci Abstr* 24:1891.
- Hetherington TE, Lombard RE (1983) Electromyography of the opercularis muscle of *Rana catesbeiana*: an amphibian tonic muscle. *J Morphol* 175:17–26.
- Hoover N, Weathington N, Weaver AL, Hooper SL (1999) EJP amplitude shows large random variation in several intrinsic pyloric muscle in *Panulirus*. *Soc Neurosci Abstr* 25:1642.
- Hoyle G (1953) “Slow” and “fast” nerve fibres in locusts. *Nature* 172:165.
- Hoyle G (1983) *Muscles and their neural control*. New York: Wiley.
- Huang EP, Stevens CF (1997) Estimating the distribution of synaptic reliabilities. *J Neurophysiol* 78:2870–2880.
- Johnston W, Wu SM-S (1995) *Foundations of cellular neurophysiology*. Cambridge, MA: MIT.
- Koehnle TJ, Morris LG, Thuma JB, Hooper SL (1997) Motor activity of the pyloric and cardiac sac network-innervated cv1 muscle. *Soc Neurosci Abstr* 23:477.
- Levin JE, Miller JP (1996) Broadband neural encoding in the cricket cercal sensory system enhanced by stochastic resonance. *Nature* 380:165–168.
- Lingle C (1980) The sensitivity of decapod foregut muscles to acetylcholine and glutamate. *J Comp Physiol* 138:187–199.
- Lisman JE (1997) Bursts as a unit of neural information: making unreliable synapses reliable. *Trends Neurosci* 20:38–43.
- Maynard DM, Dando MR (1974) The structure of the stomatogastric neuromuscular system in *Callinectes sapidus*, *Homarus americanus*, and *Panulirus argus* (decapoda crustacea). *Philos Trans R Soc Lond Biol Sci* 268:161–220.

- Morris LG, Hooper SL (1997) Muscle response to changing neuronal input in the lobster (*Panulirus interruptus*) stomatogastric system: spike number versus spike frequency dependent domains. *J Neurosci* 17:5956–5971.
- Morris LG, Hooper SL (1998) Muscle response to changing neuronal input in the lobster (*Panulirus interruptus*) stomatogastric system: slow muscle properties can transform rhythmic input into tonic output. *J Neurosci* 18:3433–3442.
- Morris LG, Hooper SL (2001) Mechanisms underlying stabilization of temporally summated muscle contractions in the lobster (*Panulirus*) pyloric system. *J Neurophysiol* 85:254–268.
- Msghina M, Govind CK, Atwood HL (1998) Synaptic structure and transmitter release in crustacean phasic and tonic motor neurons. *J Neurosci* 18:1374–1382.
- Msghina M, Millar AG, Charlton MP, Govind CK, Atwood HL (1999) Calcium entry related to active zones and differences in transmitter release at phasic and tonic synapses. *J Neurosci* 19:8419–8434.
- Russell DF, Wilkens LA, Moss F (1999) Use of behavioural stochastic resonance by paddle fish for feeding. *Nature* 402:291–294.
- Selverston AI, Russell DF, Miller JP, King DG (1976) The stomatogastric nervous system: structure and function of a small neural network. *Prog Neurobiol* 7:215–290.
- Sen K, Jorge-Rivera JC, Marder E, Abbott LF (1996) Decoding synapses. *J Neurosci* 16:6307–6318.
- Sherman SM (2001) Tonic and burst firing: dual modes of thalamocortical relay. *Trends Neurosci* 24:122–126.
- Simmons PJ (2000) Intrinsic noise at synapses between a wing hinge stretch receptor and flight motor neurons in the locust. *J Exp Biol* 204:127–138.
- Stevens CF, Wang YY (1995) Facilitation and depression at single central synapses. *Neuron* 14:795–802.
- Stevens CF, Zador AM (1998) Input synchrony and the irregular firing of cortical neurons. *Nat Neurosci* 1:210–217.
- Swadlow HA, Gusev AG (2001) The impact of “bursting” thalamic impulses at a neocortical synapse. *Nat Neurosci* 4:402–408.

## APPENDIX

### Temporally summated declining exponentials have equal areas regardless of spike patterning

Figure 13 shows three idealized EJPs consisting of amplitudes  $a_1$ ,  $a_2$ , and  $a_3$ , each of which declines with the same time constant  $\tau$  (for the muscles shown here,  $\tau$  does not vary appreciably with summated contraction amplitude). In this figure the spikes inducing the EJPs occur at sufficiently high frequency that the EJPs temporally summate. The area under the summated EJPs can be calculated as follows:

Area from 0 to  $t_1$ : this is the area under a declining exponential of amplitude  $a_1$  between  $t_1$  and 0, or

$$A_1 = \int_0^{t_1} a_1 e^{-t/\tau} dt = -a_1 \tau e^{-t/\tau} \Big|_0^{t_1} = a_1 \tau (1 - e^{-t_1/\tau}).$$

Area from  $t_1$  to  $t_2$ : this is the area of a declining exponential of amplitude  $a_2$  plus the amplitude of the first exponential at  $t_1$ . At  $t_1$  the amplitude of the first exponential is  $a_1 e^{-t_1/\tau}$ . The area is thus:

$$\begin{aligned} A_2 &= \int_0^{t_2-t_1} (a_2 + a_1 e^{-t/\tau}) e^{-t_1/\tau} dt \\ &= -(a_2 + a_1 e^{-t/\tau}) \tau e^{-t_1/\tau} \Big|_0^{t_2-t_1} \\ &= \tau [a_2 (1 - e^{-(t_2-t_1)/\tau}) + a_1 (e^{-t_1/\tau} - e^{-t_2/\tau})] \end{aligned}$$

(the integral is taken between  $t_2$  and  $t_1$  and 0 because from the point of view of this EJP,  $t_1$  is its time 0).

Area from  $t_2$  to  $t_\infty$ : this is the area of a declining exponential of amplitude  $a_3$  plus the amplitude of the first exponential at  $t_2$  plus the amplitude of the second exponential at time  $t_2$ . At  $t_2$  the amplitude of the first exponential is  $a_1 e^{-t_2/\tau}$  and the amplitude of the second exponential is  $(a_2 + a_1 e^{-t_1/\tau}) e^{-(t_2-t_1)/\tau} = a_2 e^{(t_1-t_2)/\tau} + a_1 e^{-t_2/\tau}$ . The area is thus:

$$\begin{aligned} A_3 &= \int_0^\infty (a_3 + a_2 e^{(t_1-t_2)/\tau} + a_1 e^{-t_2/\tau}) e^{-t/\tau} dt \\ &= -(a_3 + a_2 e^{(t_1-t_2)/\tau} + a_1 e^{-t_2/\tau}) \tau e^{-t/\tau} \Big|_0^\infty \\ &= \tau (a_3 + a_2 e^{(t_1-t_2)/\tau} + a_1 e^{-t_2/\tau}) \end{aligned}$$

(the integral is taken between  $\infty$  and 0 because from the point of view of this exponential,  $t_2$  is its time 0).

Total area ( $A_T$ ): summing  $A_1$ ,  $A_2$ ,  $A_3$  and rearranging terms gives

$$\begin{aligned} A_T &= \tau (a_1 - a_1 e^{-t_1/\tau} + a_1 e^{-t_1/\tau} - a_1 e^{-t_2/\tau} + a_1 e^{-t_2/\tau} \\ &\quad + a_2 - a_2 e^{(t_1-t_2)/\tau} + a_2 e^{(t_1-t_2)/\tau} + a_3) \\ &= \tau (a_1 + a_2 + a_3). \end{aligned}$$

Because the area under each individual exponential is just  $\tau$  times initial amplitude, this is the same area as the total area under the three exponentials were they sufficiently separated that they did not temporally summate. The area underneath declining exponentials is thus the same regardless of the frequency of the events that trigger them, and hence depends only on event num-

ber. Compare this to compound amplitude, which depends on the amount of temporal summation that occurs, and thus depends on event frequency as well as event number.

### Using generally accepted membrane resistivities, pyloric muscle fibers could contain many or few length constants

Length constant ( $\lambda$ ) is  $\sqrt{aR_m/2R_i}$ , where  $a$  is fiber radius, and  $R_m$  and  $R_i$  are membrane and intracellular (axial) specific resistivity, respectively. The input resistance ( $R_n$ ) of a sealed end cable in which current is injected at one end is  $R_n = \sqrt{R_m R_i} / (2\pi a)^{1.5} \tanh(l/\lambda)$ , where  $l$  is cable length (Johnston and Wu, 1995). Substituting  $\lambda = \sqrt{aR_m/2R_i}$  and rearranging terms gives  $\tanh(l/\sqrt{aR_m/2R_i}) = \sqrt{R_m R_i} / (2\pi a)^{1.5} \pi R_n$ . Pyloric muscle fibers are  $\sim 1$  cm in length and  $1 \times 10^{-2}$  to  $2.5 \times 10^{-2}$  cm in diameter (Maynard and Dando, 1974) (our unpublished observations). Assuming an  $R_i$  of 100  $\Omega$  cm and using an average radius of  $0.875 \times 10^{-2}$  cm gives  $\tanh(1/\sqrt{0.00875R_m/200}) = \sqrt{50R_m}/0.00875^{1.5} \pi R_n$ . Pyloric muscle  $R_n$ s are on the order to  $10^5$  to  $10^6$   $\Omega$  (E. Marder, personal communication). Numerically solving for  $R_m$  gives values ranging from 1321 (for  $R_n = 10^5$ ) to 47,592 (for  $R_n = 10^6$ )  $\Omega$  cm<sup>2</sup>. The latter value is higher than most estimates of  $R_m$ , which is generally believed to be between  $10^3$  and  $10^4$   $\Omega$  cm<sup>2</sup>. Using  $R_m$  values of 1321 and  $10^4$  gives  $\lambda$  values of 0.24 to 0.66 cm; using an  $R_m$  value of  $2 \times 10^4$  gives a  $\lambda$  of 0.94 cm. The diameter, length, and input resistance of pyloric muscle fibers are thus such that, within the range of generally accepted membrane resistivity values, they could contain many or few length constants. Compare this to a 2  $\mu$ m diameter axon, which would have (using again an  $R_i$  of 100  $\Omega$  cm)  $\lambda$  values of 0.022 and 0.071 cm for  $R_m$  values of  $10^3$  and  $10^4$ , respectively. As such, a 1 cm axon contains many length constants for all generally accepted membrane resistivities.

### Damage induced by sequentially moving a voltage-recording electrode towards the site of current injection can only overestimate length constant

Sequential reimpalement of a muscle fiber might be expected to induce damage and reduce the membrane resistance at the sites of impalement. Given that  $\lambda = \sqrt{aR_m/2R_i}$ , it might be initially assumed that this reduction in  $R_m$  would result in an underesti-

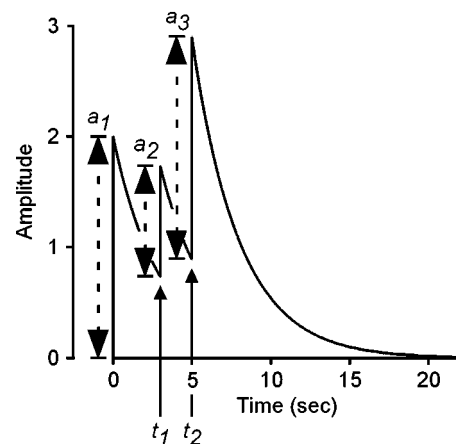
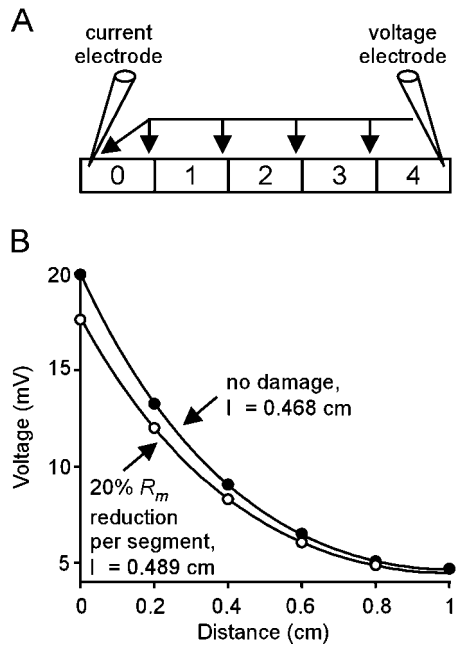


Figure 13. The area under temporally summing declining exponentials does not depend on interspike interval. Three exponentials of amplitude  $a_1$ ,  $a_2$ , and  $a_3$  occur at times 0,  $t_1$ , and  $t_2$ . The area underneath the summed exponentials does not depend on  $t_1$  and  $t_2$ .



**Figure 14.** Damage that occurs when a voltage-recording electrode is moved sequentially toward a current-injecting electrode only overestimates cable length constant. **A**, Model setup. A 1 cm, five-compartment cable with a current-injecting electrode in compartment 0. A voltage-recording electrode is sequentially moved from compartment 4 to 3 to 2 to 1 to 0. At each voltage-recording electrode placement, a current pulse is injected through the current-injecting electrode, and the resultant voltage change is measured by the voltage-recording electrode. **B**, Plot of voltage versus distance assuming no damage is done when the voltage-recording electrode is moved (closed circles), and assuming that compartment  $R_m$  is reduced by 20% each time the voltage-recording electrode is removed from the compartment (open circles). Because the reduction in measured voltage change becomes larger as the voltage-recording electrode approaches the current-injecting electrode, damage results in an overestimate of cable length constant.

mate of  $\lambda$ . This misconception would arise because of a failure to appreciate that the damage does not arise globally throughout the membrane of the fiber, but rather occurs at specific, localized regions in it. To make this clear, consider the five-compartment fiber shown in Fig. 14A. The fiber is 1 cm long and has a radius of  $0.875 \times 10^{-2}$  cm, an internal resistivity of  $100 \Omega \text{ cm}$ , and a membrane resistivity of  $5003 \Omega \text{ cm}^2$ . Substitution into  $\lambda = \sqrt{aR_m/2R_i}$  and  $R_n = \sqrt{R_m R_i}/2/(\pi a^{1.5} \tanh(l/\lambda))$  shows that  $\lambda = 0.468$  cm and  $R_n = 2 \times 10^5 \Omega$ .

The current injecting electrode is placed at the left end of compartment 0. The voltage recording electrode is sequentially moved from compartment 4 to compartment 0. In compartments 4 through 1 the voltage recording electrode is always placed at the

right end of the compartment. In compartment 0 it is placed first at the right and then at the left end of the compartment. Voltage is thus sequentially measured at 1, 0.8, 0.6, 0.4, 0.2, and 0 cm from the current-injecting electrode. The current-injecting electrode injects 100 nA during each impalement of the voltage recording electrode, and the membrane potential changes recorded at each site are used to calculate  $\lambda$ .

The top line (filled circles) in Fig. 14B shows data for the case in which the voltage recording electrode did not damage the muscle fiber. The line is a best fit to  $V = V_0 \cosh(l/\lambda - d/\lambda)/\cosh(l/\lambda)$ , which gives the decline in voltage along a sealed end fiber; for these data the fit gives  $\lambda = 0.468$  cm and a  $V_0 = 20$  mV, which is correct ( $100 \text{ nA} \times 2 \times 10^5 \Omega = 20 \text{ mV}$ ). The lower line (open circles) in Fig. 14B shows the data for a case in which each time the voltage recording electrode was withdrawn, the membrane resistivity of that compartment was reduced by 20%. For the first recording (at the end of compartment 4), because the electrode had not yet been removed, the resistivity of the compartment was the same as in the control, and thus the voltage change was the same. However, the voltage drop measured in each subsequent compartment is less than that in the undamaged case because current is being lost through the damaged membranes of the more distal compartments. As a result, in the damaged case the data are very similar to the undamaged case at the distant, earlier impalements, but become progressively less than the undamaged case as the voltage recording electrode is moved toward the current injecting electrode. Thus, if electrode withdrawal reduces local  $R_m$ , sequential impalement from the distal end of a fiber will result in an overestimate of  $\lambda$  (the curve fit to the 20% damage data gives  $\lambda = 0.489$  cm, a 5% increase). However, the error is relatively small for even substantial  $R_m$  decreases; a 50% decrease in  $R_m$  with each electrode withdrawal results in an overestimate of only 12%.

It is fortuitous that these errors are small, because these simulations also suggest that determining if damage is occurring in multiple impalement experiments can be difficult. The damage induced increases in  $R_m$  decrease  $R_n$  (in the 20% case by the end of the sequential impalements the  $R_n$  of the fiber is only  $1.78 \times 10^5 \Omega$ ), and in simulations this decrease in  $R_n$  is obvious because the current-injecting electrode can simultaneously measure voltage (the electrode has zero resistance). However, in real experiments, where the voltage-recording electrode is often the only reliable measure of voltage changes, this signal is unavailable. The damage-induced  $R_m$  decreases also induce variation from the perfect voltage-distance dependence given by  $V = V_0 \cosh(l/\lambda - d/\lambda)/\cosh(l/\lambda)$ . However, these decreases in goodness of fit are much too small to use to determine whether damage is occurring; in even the 50% damage case  $R^2$  was 0.99.